

Scramjet with MHD Controlled Inlet

E.G. Sheikin, A.L. Kuranov

*Hypersonic Systems Research Institute of LENINETZ Holding Company
St. Petersburg, Russia*

1. Introduction

Nowadays potentialities of MHD technology to control scramjet performance are discussing widely. There are two well known schemes that are proposed for the MHD control in the scramjet. The first scheme is often titled as the “MHD-bypass scramjet”^{1,2}. In this scheme the MHD generator, disposed upstream of the combustion chamber, transforms part of the flow enthalpy to electric power and then the electric power is transferred to the MHD accelerator disposed downstream of the combustion chamber. This scheme allows one to improve the scramjet performance if parameters of the MHD systems are chosen in a proper way. The second scheme for the MHD control in the scramjet is realization of MHD controlled inlet. MHD influence on the external flow in the scramjet inlet leads to modification of the flow field. This method of control can be used to improve the inlet characteristics at off-design conditions. In particular, in conditions when the flight Mach number M_∞ is less than design Mach number M_d the MHD control allows one to increase the air capture in the inlet^{3,4}. According to Ref.^{4,5} characteristics of MHD controlled inlet significantly depend on the magnetic field orientation, characteristics of MHD generator and on the shape and position of the region of MHD interaction.

In conditions of the scramjet inlet the static temperature of a flow is insufficient to provide its equilibrium conductivity. So, to ensure the MHD interaction in the scramjet inlet we have to use nonequilibrium methods of plasma creation. Thus, in the MHD controlled inlet a part of the power produced by the MHD generator needs to be spent on sustaining a nonequilibrium conductivity of the flow. In order to determine the position and the shape of the ionized region it is necessary to take into account features of an ionizer and configuration of a magnetic field. E-beam will be considered as an ionizer for the MHD controlled inlet, because it is characterized by minimal power spent on sustaining any given flow conductivity⁶.

Possible configurations of magnetic fields which can be realized in the MHD controlled inlet will be considered in the paper. Algorithm for defining the shape of an ionized region at arbitrary configuration of a magnetic field and any given area of the e-beam input through the inlet surface will be presented in the paper. Characteristics of the MHD controlled inlet will be investigated for various configurations of magnetic field and various features of the ionized region. As a base for the inlet geometry the two-shock inlet with the total turning angle of 15° and the Mach design number $M_d=10$ is chosen. The scheme of the inlet is shown in Fig.1. Where, $\theta_1=6.5^\circ$, $\theta_2=8.5^\circ$ and $\theta_N=\theta_1+\theta_2=15^\circ$.

It is known, that positive effects of MHD control such as the air capture increase are usually accompanied by negative effects such as the total pressure losses. Thus, only considering the total scheme of the scramjet with the

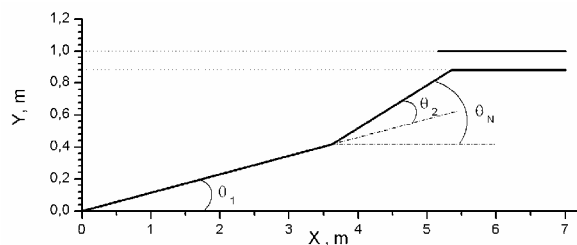


Fig.1. Geometry of inlet used in calculations.

MHD controlled inlet allows one to estimate the efficiency of the MHD control in the scramjet. In analyzing the scramjet with the MHD controlled inlet we will assume that all the power produced by the MHD generator in the MHD controlled inlet except the power spent on the flow ionization is transferred to the MHD accelerator located downstream of the combustion chamber. One can see that this propulsion combines two schemes mentioned above: the MHD controlled inlet and the MHD-bypass scramjet.

2. Possible Configurations of Magnetic Field in the MHD Controlled Inlet

The magnetic field is assumed to be generated by superconducting electromagnet. It is evident that the magnet needs to be located in the body of the scramjet inlet, because a location of any part of a magnet in a flow outside the body can increase the drag of the flight vehicle and in addition it can lead to destruction of the magnet. One variant of location of superconducting cable, which allows one to realize the MHD influence on the flow in the inlet, is shown in Fig.2. In this case the magnetic field is produced by a current which has a profile adapting both to

the construction of the flight vehicle and the requirements for the MHD generator which controls the flow in the inlet. In the figure the current is not closed. Its prolongation can engage the isolator which is located upstream of the combustion chamber, the combustion chamber and the part of the scramjet downstream of the combustion chamber. The magnetic field in the listed subsystems of the scramjet in principle can be used to control the internal flow in the scramjet in order to improve the scramjet performance. The scheme of the scramjet with MHD bypass can be used for the purpose. The current in the plane of its cross-section in principle can be shaped in any way. We consider only two profiles of current: rectangular and circular ones. Possible locations of electrodes are shown schematically in Fig.2b. The electrodes denoted in the figure by number 1 and by number 2 can be used in the MHD controlled inlet both jointly and separately.

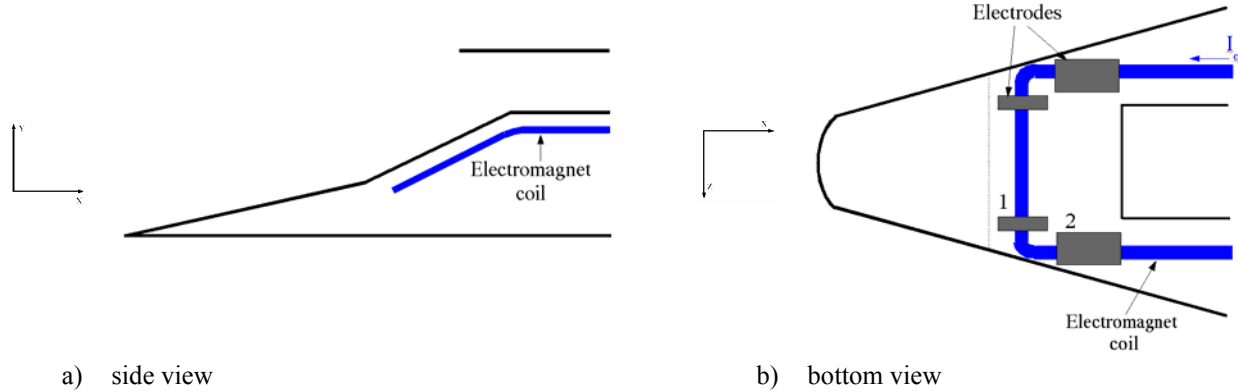


Fig.2 Possible configuration of an electromagnet coil adapting to the construction of the scramjet inlet

In order to calculate the magnetic field in the region of MHD interaction we use the noninductive approach, conventional for conditions of MHD generator. This approach corresponds to magnetic Reynolds number $Re_m \ll 1$. In this case a magnetic field induced by a current in the plasma can be neglected in comparing with the magnetic field created by the current in the electromagnet coil. The magnetic field distribution is calculated in using Maxwell's equations. The steady state equations are considered for which: $\text{rot } \mathbf{B} = \mu \mathbf{j}_c$, $\text{div } \mathbf{B} = 0$, where \mathbf{B} is the magnetic induction vector, \mathbf{j}_c is the current density in the electromagnet coil, μ is the magnetic permeability of a medium. In calculations we suppose $\mu = \mu_0 = 4\pi \cdot 10^{-7} \text{ N/A}^2$. To determine the magnetic field we introduce the vector potential \mathbf{A} , which is connected with the magnetic field by the ratio: $\mathbf{B} = \text{rot } \mathbf{A}$. Equations for Cartesian components of the vector potential have a form of Poisson's equation:

$$\Delta A_i = \mu j_{ci}, \quad i = x, y, z \quad (1)$$

If we know the current density in the electromagnet coil, for example, function $j_{cz}(x, y)$, then solution of equations (1), correspondingly for A_z , can be obtained in the next form⁷:

$$A_z(x, y) = \frac{1}{2\pi} \int_{-\infty}^{\infty} \int_{-\infty}^{\infty} \mu j_{cz}(\xi, \eta) \ln \frac{1}{\sqrt{(x-\xi)^2 + (y-\eta)^2}} d\xi d\eta \quad (2)$$

Equations for other components of the vector potential have the same form.

The magnetic flux density can be determined from the vector potential by using the evident equations:

$$B_x = \frac{\partial A_z}{\partial y} - \frac{\partial A_y}{\partial z}, \quad B_y = \frac{\partial A_x}{\partial z} - \frac{\partial A_z}{\partial x}, \quad B_z = \frac{\partial A_y}{\partial x} - \frac{\partial A_x}{\partial y} \quad (3)$$

The electrodes can be placed both on the surface of the flight vehicle and in the plane located angularly to the surface of the flight vehicle. Schematically possible configurations of electromagnet coils and MHD electrodes are shown in Figs.3,4. Fig.3 corresponds to the region with electrodes which are marked by number 2 in Fig.2b. Fig.4 corresponds to the region with electrodes which are marked by number 1 in Fig.2b.

In Ref.^{3,4} it is shown that positive effect of MHD control in the MHD controlled inlet at $M_\infty > M_d$ is achievable in a wide range of variation of such characteristics as the magnetic field orientation and a configuration of the region of MHD interaction. On the other hand in case of $M_\infty < M_d$ the effect of MHD control depends significantly on the magnetic field orientation. That is why in choosing the magnetic field configuration it is more reasonable to satisfy the requirements for MHD control in the inlet at off-design conditions for $M_\infty < M_d$. According to Ref.⁴ the more significant positive effect of MHD control in the inlet at $M_\infty < M_d$ consists in increasing the air capture. In order to effectively increase the air capture in the MHD controlled inlet it is necessary to organize the MHD influence on the flow in such a way that the Lorentz force projection directed to the inlet body receives a

maximal value⁵. The Lorentz force is defined by the relation $\mathbf{f} = \mathbf{j} \times \mathbf{B}$, where \mathbf{j} is the current density in the region of MHD interaction, which is determined by the generalized Ohm's law $\mathbf{j} + \mu_e (\mathbf{j} \times \mathbf{B}) = \sigma (\mathbf{E} + \mathbf{v} \times \mathbf{B})$, where μ_e is the electron mobility, \mathbf{E} is the electric field intensity, σ is the flow conductivity. So requirements for the Lorentz force make some requirements for configuration of the magnetic field and the region of MHD interaction.

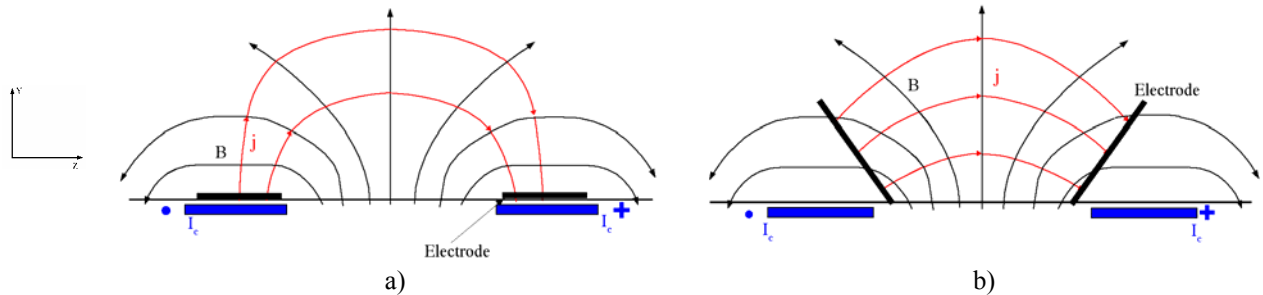


Fig.3 Configuration of magnetic field and MHD currents corresponding to location of electrodes marked in Fig.2b by number 2.

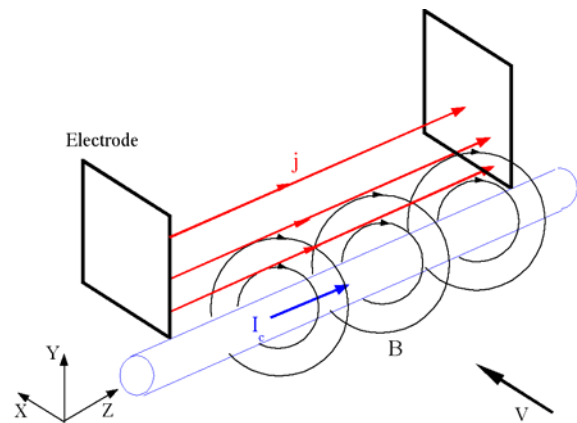


Fig.4. Configuration of magnetic field and MHD currents corresponding to location of electrodes in Fig.2b marked by number 1

A part of the MHD controlled inlet with two types of conductors producing magnetic field is shown schematically in Fig.5. We consider conductors with circular and rectangular cross-sections which carry the current I_c along the axis OZ . Parameters which determine the value and the space distribution of magnetic field are shown in Figs.5a,b. They are: position (x_0, y_0) of a conductor center, magnitude of the current I_c , width h and height d for the rectangular conductor and also angle θ_c for orientation of the conductor plane relatively to the x axis. In case of conductor with a circular cross section a magnetic field outside the conductor depends upon the distance from the point (x_0, y_0) and the value of I_c and doesn't depend on the radius of the conductor. In case of a rectangular conductor with $(d \ll h)$ the magnetic field distribution practically doesn't depend upon the d value. The magnetic field distributions in the MHD controlled inlet for conductors with rectangular and circular cross-

sections are compared in the Fig.6. It is easy to see that near the inlet surface the magnetic fields are significantly different. In moving away the surface the difference between the magnetic fields is reduced.

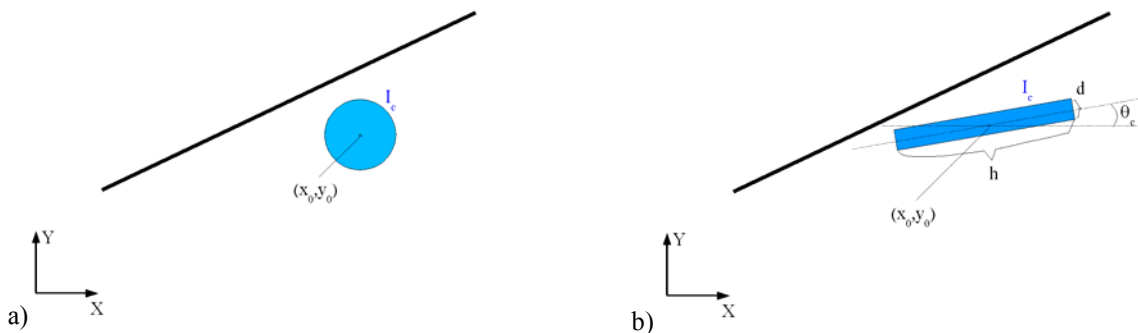


Fig.5 Part of the MHD controlled inlet with currents producing magnetic field

3. Shape of Ionized Region in the Nonequilibrium MHD Generator

In our considerations the electron beam is ionizer which produces the nonequilibrium conductivity of the flow in the scramjet inlet. Estimations show that in typical for the MHD controlled inlet conditions a magnitude of

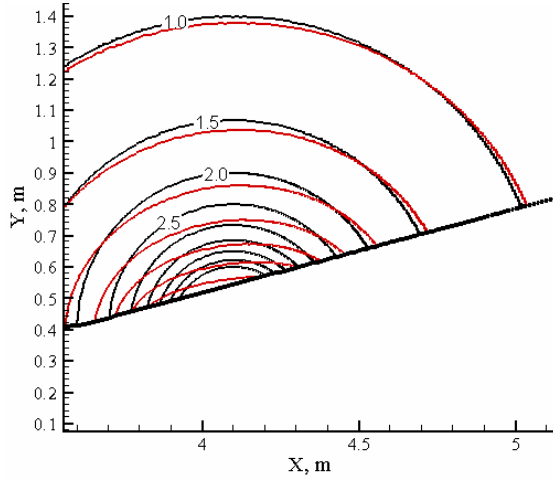


Fig.6 Contours of magnetic flux density for two various currents. Black lines correspond to the circular conductor, red lines correspond to the rectangular current with $h=0.5\text{m}$, $\theta_c=8^\circ$; $x_0=0.4\text{m}$, $y_0=4.1\text{m}$.

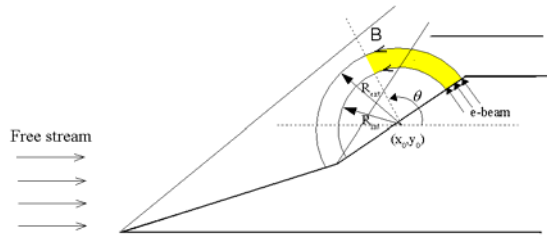


Fig.7 Sketch for MHD controlled inlet with circular magnetic field.

space location of e-beam in the MHD controlled inlet is shown in Fig.7. This situation corresponds to magnetic field produced by a conductor with a circular cross-section centered at the point (x_0, y_0) . In this case $B_y/B_x = -(x-x_0)/(y-y_0)$. Thus solution of equation (4)

has the form: $(x-x_0)^2 + (y-y_0)^2 = R^2$. So in these conditions electrons in the e-beam move along the concentric circles. The geometrical locus of the region of nonequilibrium ionization can be characterized by the center position (x_0, y_0) , magnitudes of external R_{ext} and internal R_{int} circles and the angle θ which determines the electrons ranges in the flow. In case of more complicated configuration of magnetic field a shape of a region of nonequilibrium ionization will be more complicated too. Fig.8 demonstrates possible shape of ionized region which can be realized in the MHD controlled inlet in which the magnetic field is generated by two antiparallel currents. The height of the ionized region depends on the density of a flow and on the initial energy of electrons in the e-beam. In principle, by changing the energy of e-beam depending on its location on the inlet surface one can obtain arbitrary shape of the ionized region. In the paper we will consider the depth of the e-beam penetration as a parameter which can be varied in calculations.

the Larmor radius $r_L = \frac{m_e v_e}{eB}$ for electrons of the e-beam is

significantly less than the path length of the electrons between elastic collisions, here m_e is electron mass, v_e is a velocity of electron, e is electron charge. Therefore the electrons in the e-beam propagate in the flow practically along the magnetic field lines. So equation defining the electron trajectory will be the same as equation for the magnetic field lines:

$$\frac{dx}{B_x} = \frac{dy}{B_y} = \frac{dz}{B_z}$$

Depth of penetration of electrons in the flow depends upon the flow density and initial energy of electrons. So, a location and proportions of the region of the nonequilibrium conductivity in the flow depend on the magnetic field configuration, the e-beam characteristics and the flow characteristics. We will consider in the paper configurations in which the magnetic field is produced by a current or a system of currents directed along the OZ axis. In this case the magnetic field has only two components $B_x(x, y)$ and $B_y(x, y)$. Differential equation for magnetic field line and correspondingly the differential equation for a trajectory of electrons from e-beam which are passing through a point (x_1, y_1) has the form:

$$\frac{dy}{dx} = \frac{B_y(x, y)}{B_x(x, y)} \quad (4)$$

with the boundary condition $y(x=x_1)=y_1$. The curves passing through the points bounding the area on the inlet surface that the e-beam is traversed through will define bounds of region of nonequilibrium ionization. It is evident that shape of ionized region significantly depends on configuration of magnetic field and location of e-beam in the inlet. Possible

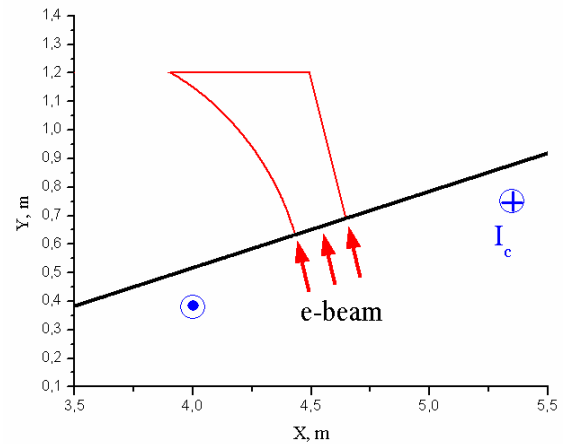


Fig.8. Possible shape of ionized region in the MHD controlled inlet with magnetic field produced by two antiparallel conductors

4. Investigation of MHD Controlled Inlet with Various Configurations of Magnetic Field.

In studying the MHD controlled inlet we assume that the power density q_i deposited by an e-beam in the flow for creation of the nonequilibrium conductivity is a constant in the ionized region. The ionization degree in the flow and its conductivity are calculated in using approximating functions from Ref.³. Flow field in the MHD controlled inlet is calculated in 2D Euler approach. Stationary mode is considered, such as:

$$\begin{aligned}\frac{\partial \rho v_x}{\partial x} + \frac{\partial \rho v_y}{\partial y} &= 0, \\ \frac{\partial (\rho v_x^2 + p)}{\partial x} + \frac{\partial \rho v_x v_y}{\partial y} &= f_x, \\ \frac{\partial (\rho v_y^2 + p)}{\partial y} + \frac{\partial \rho v_x v_y}{\partial x} &= f_y, \\ \frac{\partial (e + p) v_x}{\partial x} + \frac{\partial (e + p) v_y}{\partial y} &= q_g + q_r,\end{aligned}\tag{5}$$

where $e = \rho (c_v T + (v_x^2 + v_y^2)/2)$, $p = R\rho T$, $q_g = \mathbf{j} \cdot \mathbf{E}$, parameters ρ , v , p , and T are correspondingly the density, the velocity, the pressure and the temperature of a flow, f_x and f_y are corresponding projections of the Lorentz force. The quantity q_r included in a right side of Eq.5 determines the power released into the flow as a result of a recombination of charged particles. The ideally sectioned Faraday MHD generator, for which $\mathbf{j} = (0, 0, j_z)$ is considered. We assume that magnetic field has two components $\mathbf{B} = (B_x, B_y, 0)$. It is easy to show that in this case the MHD interaction is characterized by relations:

$$\begin{aligned}f_x &= -(v_x B_y - v_y B_x + E_z) \sigma B_y, \\ f_y &= (v_x B_y - v_y B_x + E_z) \sigma B_x, \\ q_g &= (v_x B_y - v_y B_x + E_z) \sigma E_z\end{aligned}\tag{6}$$

The value E_z is considered as a parameter which can be varied in calculations. Let's mention that $E_z=0$ corresponds to the short circuit regime of the MHD system. By varying the E_z value we can change a regime of MHD interaction.

Negative values of q_g correspond to the MHD generator and positive values of q_g correspond to the MHD accelerator. One can see from equations (6) that in the case when the flow field and the magnetic field are nonuniform in the region of an MHD interaction the MHD effect will be nonuniform too. In all the calculations we make a control of the total power produced by the MHD generator $W_g = -\int_{S_i} q_g dx dy$, where S_i is the region of MHD

interaction. The self-sustained operational mode of the MHD generator is realized when the power spent on the flow ionization $W_i = \int_{S_i} q_i dx dy$ is less than the power produced by

the MHD generator: $W_i < W_g$. The values W_g and W_i are normalized on the unit of the length in the transverse direction z .

In order to define what profile of a conductor (circular or rectangular) producing a magnetic field in the MHD controlled inlet is preferable to be used, computations of flow fields in the inlet were made at $M_\infty < M_d$ at fixed value of I_c . Position of magnetic field source (x_0, y_0) and also the values h and θ_c (for rectangular conductor) were varied in the computations. Width of the e-beam was varied in the computations too. Fig.9 demonstrates ratio of air captures realized in the MHD controlled inlet with magnetic field produced by currents shown in Fig.5b – φ_h , and φ_R corresponding to Fig.5a. According to Fig.9 the magnetic field produced by the circular current provides slightly greater increment of the air capture in the inlet than one produced by

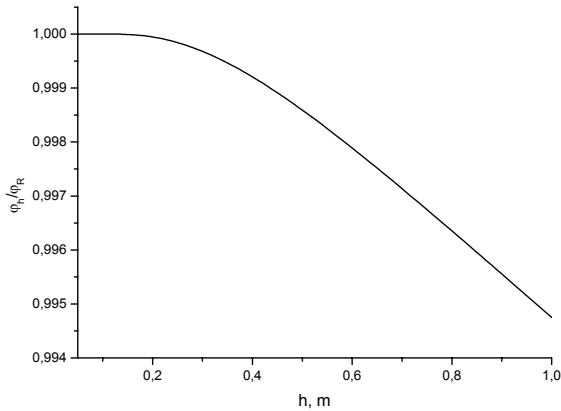


Fig.9. Ratio of air captures in the MHD controlled inlet at $M_\infty=6$, $M_d=10$, $\theta_c=9^\circ$, $x_0=4.0\text{m}$, $y_0=0.4\text{m}$

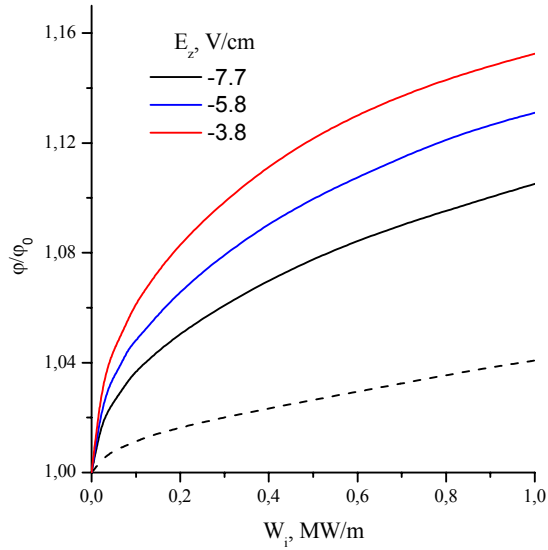


Fig.10. Relative air capture in the MHD controlled inlet at $M_\infty=6$ and free-stream dynamic pressure 75kPa

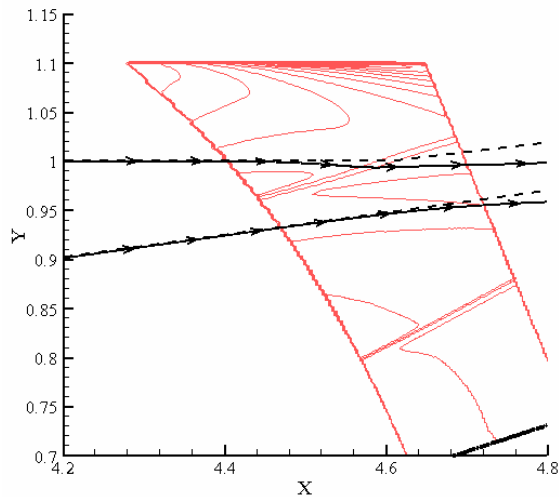


Fig.11. Contours of q_g in the MHD controlled inlet at $M_\infty=8$ and free-stream dynamic pressure 75kPa. Magnetic field is generated by two antiparallel currents

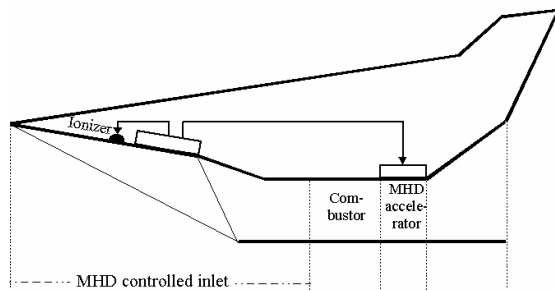


Fig.12. Scramjet with MHD controlled inlet

the rectangular current. Fig.10 demonstrates dependencies of the air capture in the MHD controlled inlet upon the power W_i spent on flow ionization at various values of E_z . Here ϕ is the air capture in the MHD controlled inlet, ϕ_0 is the air capture in the inlet without MHD control. Dashed line in Fig.10 corresponds to magnetic field generated by the circular current located at point (3.9, 0.2). Solid lines shown in Fig.10 correspond to magnetic field generated by two antiparallel currents located in points (4.2, 0.5) and (5.4, 1.1). One can see that configuration of magnetic field significantly influence on the air capture in the MHD controlled inlet. The magnetic field generated by two antiparallel currents looks more preferable for using in the scramjet inlet for flow control.

Streamlines shown in Fig.11 illustrate reasons which are responsible for increasing the air capture in the MHD controlled inlet. Dashed lines in Fig.11 correspond to streamlines in the inlet without MHD interaction. One can see that MHD control, due to the Lorentz force action, leads to deflection of the streamlines to the inlet body that result in increasing the air capture.

In order to determine integral result of MHD control we need to calculate thrust of a scramjet with MHD controlled inlet. Similarly to paper⁵ we consider the scramjet with MHD controlled inlet in assuming that all the power produced by the MHD generator, except the power spent on the flow ionization, is transferred to the MHD accelerator located downstream of the combustion chamber. Simplified scheme of the scramjet is shown in Fig.12. The nozzle located downstream of the MHD accelerator is considered as a fully expanded nozzle. The calculations are made analogously to the paper⁵. Relative thrust of the scramjet with an MHD controlled inlet depending on the power W_i spent on flow ionization is shown in Fig.13. Here the relative thrust is the thrust of the scramjet with the MHD control divided by the thrust of the scramjet without the MHD control. Dashed line in Fig.13 corresponds to magnetic field generated by the circular current and solid line shown in Fig.13 corresponds to magnetic field generated by two antiparallel currents. One can see that MHD control leads to increasing the scramjet thrust for all considered configurations of magnetic fields. The magnetic field generated by two antiparallel currents provides more significant increase of the scramjet thrust.

References

1. Sheikin E.G., "Parametric and Numerical Investigations of Scramjet with MHD Bypass" AIAA Paper 2005-1336
2. Park C., Bogdanoff D.W., and Mehta U.B., "Theoretical Performance of a Magnetohydrodynamic-Bypass Scramjet Engine with Nonequilibrium Ionization," Journal of Propulsion and Power, v19, №4, July-August 2003, p.529-537
3. Kuranov A.L. and Sheikin E.G.,

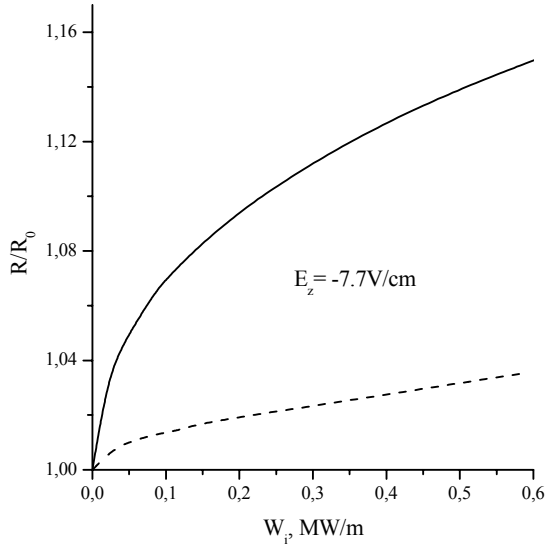


Fig.13. Relative thrust of scramjet with MHD controlled inlet at $M_\infty = 6$.

“Magnetohydrodynamic Control on Hypersonic Aircraft under “AJAX” Concept”, Journal of Spacecraft and Rockets, v40, №2, March-April 2003, p.174-182.

4. Kuranov A.L. and Sheikin E.G., “MHD control by external and internal flows in scramjet under “AJAX” concept”, AIAA paper 2003-0173.
5. Sheikin E.G. and Kuranov A.L., “MHD controlled inlet for scramjet with various configurations of magnetic field”, AIAA paper 2004-1195
6. Macheret S.O., Shneider M.N. and Miles R.B, Modeling of air plasma generation by electron beams and high-voltage pulses, AIAA 2000-2569
7. Poljanin A.D.,”Reference book on the linear equations of mathematical physics”, Moscow, “Physicomathematical Literature”, 2001 (in Russian).